MARTIN MARIETTA ENERGY SYSTEMS LIBRARIES

3 4456 0354675 9

ORNL/TM-11827

ornl

OAK RIDGE NATIONAL LABORATORY

MARTIN MARIETTA

Excess Heat Production in Composite Superconductors During Current Redistribution

Lawrence Dresner

OAK RIDGE NATIONAL LABORATORY
CENTRAL RESEARCH LIBRARY
CIRCULATION SECTION
4500N ROOM 175
LIBRARY LOAN COPY
DO NOT TRANSFER TO ANOTHER PERSON
If you wish someone else to see this report, send in name with report and the library will arrange a loan.

MANAGED BY
MARTIN MARIETTA ENERGY SYSTEMS, INC.
FOR THE UNITED STATES
DEPARTMENT OF ENERGY

This report has been reproduced directly from the best available copy.

Available to DOE and DOE contractors from the Office of Scientific and Technical Information, P.O. Box 62, Oak Ridge, TN 37831; prices available from (615) 576-8401, FTS 626-8401.

Available to the public from the National Technical Information Service, U.S. Department of Commerce, 5285 Port Royal Rd., Springfield, VA 22161.

This report was prepared as an account of work sponsored by an agency of the United States Government. Neither the United States Government nor any agency thereof, nor any of their employees, makes any warranty, express or implied, or assumes any legal liability or responsibility for the accuracy, completeness, or usefulness of any information, apparatus, product, or process disclosed, or represents that its use would not infringe privately owned rights. Reference herein to any specific commercial product, process, or service by trade name, trademark, manufacturer, or otherwise, does not necessarily constitute or imply its endorsement, recommendation, or favoring by the United States Government or any agency thereof. The views and opinions of authors expressed herein do not necessarily state or reflect those of the United States Government or any agency thereof.

ORNL/TM-11827
Dist. Category UC-220

Fusion Energy Division

EXCESS HEAT PRODUCTION IN COMPOSITE SUPERCONDUCTORS DURING CURRENT REDISTRIBUTION

Lawrence Dresner

Date Published: May 1991

Prepared for the
Superconducting Technology for
Electric Energy Systems Program
Budget Activity No. AK 06 01 00 0

Prepared by
OAK RIDGE NATIONAL LABORATORY
Oak Ridge, Tennessee 37831
managed by
MARTIN MARIETTA ENERGY SYSTEMS, INC.
for the
U.S. DEPARTMENT OF ENERGY
under contract DE-AC05-84OR21400

MARTIN MARIETTA ENERGY SYSTEMS LIBRARIES

3 4456 0354675 9

CONTENTS

ABSTRACT v
1. INTRODUCTION 1
2. GENERAL FORMULATION 1
3. SLAB CONDUCTOR 3
4. CYLINDRICAL CONDUCTOR 5
5. RECTANGULAR CONDUCTOR 7
REFERENCES 11
Appendix A. CALCULATION FOR EQ. (12) 13
Appendix B. CALCULATION FOR EQ. (17a) 15
Appendix C. CALCULATION FOR EQ. (18) 17

ABSTRACT

Immediately after a large conductor with segregated matrix and superconductor is driven normal, the transport current is confined to the vicinity of the superconductor; thus, the Joule power is initially much larger than it would be if the current density were uniform. Subsequently, the current diffuses throughout the matrix and eventually fills it uniformly, so that the excess Joule power gradually falls to zero. This paper presents simple formulas for the time-integrated excess Joule power (the excess Joule heat) produced in conductors of various shapes with various dispositions of matrix and superconductor.

1. INTRODUCTION

Very large composite conductors with segregated matrix and superconductor have been proposed recently for a variety of purposes, for example, energy storage magnets,[1] fusion magnets,[2] and space applications.[3] Typically, such conductors operate with currents in the range from 30 to 100 kA, are of the order of 2.5 to 5 cm in diameter, and consist of large blocks of aluminum in which much smaller superconductors are embedded.

The segregation of the aluminum matrix and the superconductor has a deleterious effect on the stability of the conductor. When the superconductor is first normalized, the current enters the matrix but is confined to the vicinity of the superconductor. The Joule power is then very high. Thereafter, the current diffuses throughout the matrix, tending toward a state of uniform current density. In this uniform state, the Joule power is much lower than at the start.

The relaxation time of current redistribution is typically some tens of milliseconds. So the excess Joule power (over the uniform state) appears as a short pulse immediately following normalization. For magnets that are not fully cryostable, this pulse reduces the stability margin. It has already been shown to have a strong effect on the propagation velocity.[4–6]

The purpose of this report is to calculate the magnitude of this excess Joule heat pulse for conductors of several shapes having various dispositions of superconductor in the matrix. The goal is simple, easily evaluated formulas for the excess Joule heat.

2. GENERAL FORMULATION

Let the axes so be chosen that the z-axis points along the conductor in the direction of flow of the transport current I. Let Ω denote the cross section of the conductor in the (x,y) plane and let Ω_0 denote the portion of Ω in which the transport current is initially confined. At $t = 0$, imagine this confinement to be abrogated. The transport current then diffuses transversely, tending toward a state of uniform current density. During this redistribution, the current density J obeys the diffusion equation

$$\frac{\partial J}{\partial t} = \frac{\rho}{\mu_0}\nabla^2 J. \tag{1}$$

We wish to solve Eq. (1) under the boundary and initial conditions

$$J(\hat{r},\infty) = I/\Omega_0 \text{ everywhere in } \Omega\,, \tag{2a}$$

$$J(\hat{r},0) = \begin{cases} I/\Omega_0 \text{ in } \Omega_0 \\ 0 \quad \text{elsewhere in } \Omega \end{cases}, \tag{2b}$$

$$\int_\Omega J(\hat{r},t)\,d\omega = I\,, \tag{2c}$$

where $d\omega = dx\,dy$ and $\hat{r}$ is the two-dimensional radius vector (x,y).

It proves useful to expand J in terms of certain eigenfunctions ϕ_k of the Helmholtz equation in Ω, namely, those defined by the equations

$$\nabla^2\phi_k + \alpha_k^2\phi_k = 0 \text{ in } \Omega \ , \tag{3a}$$

$$\hat{n}\cdot\nabla\phi_k = 0 \qquad \text{on } \Sigma\text{, the boundary of } \Omega \ , \tag{3b}$$

where $\hat{n}$ is the outward normal to Σ. Thus we set

$$J = \frac{I}{\Omega} + \sum_{k=1}^{\infty} A_k\phi_k(\hat{r})\exp(-\rho\alpha_k^2 t/\mu_0) \ , \tag{4}$$

which satisfies Eq. (1). Equation (4) also satisfies condition (2a). It follows by well-known arguments[7] that

$$(\phi_k,\ 1) \equiv \int_\Omega \phi_k\, d\omega = 0, \tag{5a}$$

$$(\phi_k,\ \phi_m) \equiv \int_\Omega \phi_k\phi_m\, d\omega = 0 \quad (k \neq m) \ . \tag{5b}$$

With the help of Eq. (5a) we can see that Eq. (4) satisfies condition (2c). We choose the coefficients A_k to satisfy condition (2b), which can be written

$$\frac{I}{\Omega_0}\, g(\Omega_0) = \frac{I}{\Omega} + \sum_{k=1}^{\infty} A_k\phi_k \ , \tag{6}$$

where $g\Omega_0$ is the characteristic function of Ω_0, that is, the function which is 1 inside Ω_0 and 0 outside. Using Eq. (5), we find that

$$A_k = \frac{I}{\Omega_0}\frac{(\phi_k,\ g)}{(\phi_k,\ \phi_k)} \ . \tag{7}$$

The Joule power expended per unit length of conductor is

$$\int_\Omega \rho J^2 d\omega = \rho\left(\frac{I}{\Omega}\right)^2\Omega + \rho\sum_{k=1}^{\infty} A_k^2(\phi_k,\ \phi_k)\exp\left(-2\rho\alpha_k^2 t/\mu_0\right) \ . \tag{8}$$

The first term on the right in Eq. (8) is the Joule power produced when the current density is uniform throughout Ω. The second term is the excess Joule power. When integrated over t from 0 to ∞, the second term gives the excess Joule heat per unit length of conductor. Dividing the result by Ω gives Q, the excess Joule heat density:

$$Q = \frac{\mu_0}{2\Omega}\sum_{k=1}^{\infty} A_k^2(\phi_k,\ \phi_k)/\alpha_k^2 \tag{9a}$$

or

$$Q = \frac{\mu_0 I^2}{\Omega} \cdot \frac{1}{2} \sum_{k=1}^{\infty} \frac{(\phi_k, g)^2}{(\phi_k, \phi_k)\, \alpha_k^2\, \Omega_0^2} \ . \tag{9b}$$

The second factor in Eq. (9b) is a dimensionless geometric factor, the calculation of which is the goal of this paper.

3. SLAB CONDUCTOR

Nowhere in the derivation of Eq. (9b) did we make any use of the dimensionality of Ω, so Eq. (9b) applies as well to slab geometry. In a slab of thickness $2h$ centered on $z = 0$, the eigenfunctions for *reflection-symmetric* current distributions are

$$\phi_k = \cos\left(\frac{\pi k z}{h}\right) \tag{10a}$$

$$k = 1, 2, 3, \ldots$$

$$\alpha_k = \frac{\pi k}{h} \tag{10b}$$

Then $(\phi_k, \phi_k) = h$.

Interior Source. If the initial current distribution is of thickness $2a$ centered on $z = 0$, then $\Omega_0 = 2a$ and

$$(\phi_k, g) = \frac{2h}{k\pi} \sin\left(\frac{k\pi a}{h}\right) \ . \tag{11}$$

Equation (9b) now becomes

$$Q = \frac{\mu_0 I^2}{24} \cdot \frac{6}{\pi^2} \sum_{k=1}^{\infty} \frac{1}{k^2} \left[\frac{\sin(\pi k a/h)}{(\pi k a/h)}\right]^2 , \tag{12}$$

where I represents the current per unit length of the slab (see Fig. 1). A straightforward computation shows that the second factor in Eq. (12) is $(1 - a/h)^2$ (see Appendix A). Thus

$$Q = \frac{\mu_0 I^2}{24} (1 - a/h)^2 \ . \tag{13}$$

Exterior Source. Suppose the initial current distribution is confined to regions of thickness a at the outer edges of the slab (Fig. 2). If two such slabs are put in contact (top view, Fig. 3), Q will not change; for owing to the symmetry of the setup, neither slab will influence the instantaneous current distribution in the other. Now, again owing to symmetry, if we remove the parts of the conductor outside the dash-dot lines in Fig. 3, Q will not change. What is left is the same situation as shown in Fig. 1, so Eq. (13) holds as well for the slab of Fig. 2.

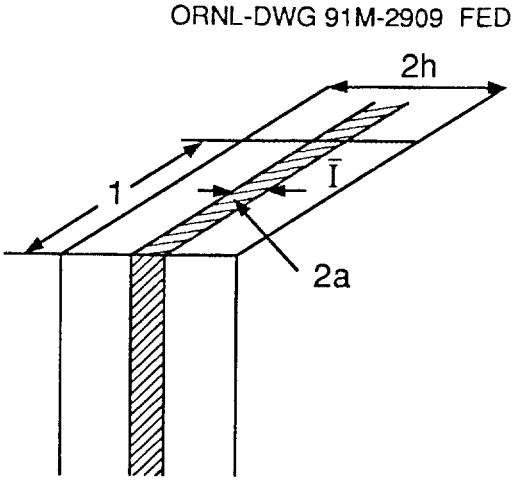

Fig. 1. Sketch of a slab conductor of thickness $2h$ with an initial current distribution of thickness $2a$ centered in the matrix.

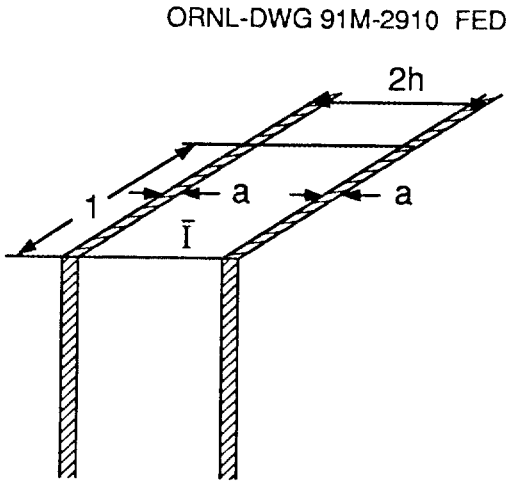

Fig. 2. Sketch of a slab conductor of thickness $2h$ with an initial current distribution confined to regions of thickness a at the outer edges.

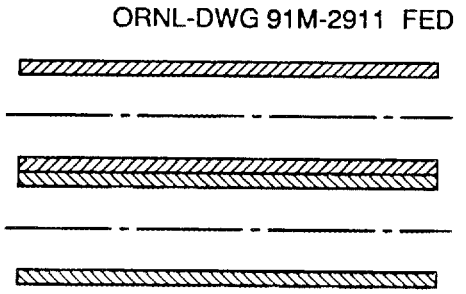

Fig. 3. Top view of two slabs of the kind shown in Fig. 2 put in contact.

4. CYLINDRICAL CONDUCTOR

In a cylinder of radius R, for current distributions that depend only on the radius (azimuthal symmetry),

$$\phi_k = J_0\left(\gamma_k \frac{r}{R}\right) \qquad k = 1, 2, 3, \ldots \tag{14a}$$

$$\alpha_k = \frac{\gamma_k}{R} \tag{14b}$$

where J_0 is the Bessel function of the first kind of order zero and γ_k is the kth root of J_1, the Bessel function of the first kind of order one. Then

$$(\phi_k, \phi_k) = \int_0^R 2\pi r\, J_0^2\left(\gamma_k \frac{r}{R}\right) dr = \pi R^2 J_0^2(\gamma_k) \quad . \tag{15}$$

Suppose Ω_0 is the annulus $R_1 < r < R_2$. Then

$$(\phi_k, g) = \int_{R_1}^{R_2} 2\pi r\, J_0\left(\gamma_k \frac{r}{R}\right) dr = \frac{2\pi R^2}{\gamma_k}\left[\frac{R_2}{R} J_1\left(\gamma_k \frac{R_2}{R}\right) - \frac{R_1}{R} J_1\left(\gamma_k \frac{R_1}{R}\right)\right] . \tag{16}$$

Thin Outer Ring. If we set $R_2 = R$ and $R_1 = R(1-\varepsilon)$, we find, in the limit as $\varepsilon \to 0$,

$$Q = \frac{\mu_0 I^2}{2\pi^2 R^2} \sum_{k=1}^{\infty} \frac{1}{\gamma_k^2} = \frac{\mu_0 I^2}{16\pi^2 R^2} \quad . \tag{17a}$$

The exact value of the sum in the middle term of Eq. (17a) is 1/8; see Appendix B for the evaluation of this sum.

When ε is not zero

$$Q = \frac{\mu_0 I^2}{16\pi^2 R^2} \cdot 8\left(\frac{1-\varepsilon}{1-\varepsilon/2}\right)^2 \sum_{k=1}^{\infty} \frac{1}{\gamma_k^2}\left[\frac{J_1(\gamma_k(1-\varepsilon))}{\varepsilon \gamma_k J_0(\gamma_k)}\right]^2 . \tag{17b}$$

Table 1 gives the second factor in Eq. (17b) as a function of ε.

Table 1. The second factor in Eq. (17b) for various ε

$\varepsilon = 1 - R_1/R = \Delta R/R$	Second factor
0	1
0.01	0.9734
0.025	0.9346
0.05	0.8716
0.10	0.7532
0.20	0.5454
0.50	0.1414
0.75	0.01631
1	0

For small values of ε (ε < 0.2), the second factor can be fitted well by the empirical expression $(1 - 4\varepsilon/3)^2$.

Inner Cylinder. In this case, we let $R_1 = 0$. Then

$$Q = \frac{\mu_0 I^2}{R^2} \cdot \frac{2}{\pi^2 (R_2/R)^2} \sum_{k=1}^{\infty} \left[\frac{J_1(\gamma_k R_2/R)}{\gamma_k^2 J_0(\gamma_k)} \right]^2 . \tag{18}$$

Shown in Table 2 are numerically calculated values for various values of R_2/R.

Table 2. The second factor in Eq. (18) for various R_2/R

R_2/R	Second factor
0.1	4.579×10^{-2}
0.2	2.861
0.3	1.897
0.4	1.257
0.5	8.059×10^{-3}
0.6	4.834
0.7	2.575
0.8	1.093
0.9	2.624×10^{-4}

The right-hand side of Eq. (18) diverges logarithmically as $R_2/R \to 0$:

$$Q \sim \frac{\mu_0 I^2}{R^2} \cdot \frac{\ln(R/R_2)}{4\pi^2} . \tag{19}$$

(For a proof, see Appendix C.)

5. RECTANGULAR CONDUCTOR

A complete set of eigenfunctions of Eqs. (3a,b) even in both x and y for the rectangle $-a < x < a$, $-b < y < b$ is

$$\phi_{km} = \cos\left(\frac{k\pi x}{a}\right)\cos\left(\frac{m\pi y}{b}\right) \tag{20a}$$

$$k, m = 0, 1, 2, 3, \ldots$$

$$\alpha_{km}^2 = \pi^2\left(\frac{k^2}{a^2} + \frac{m^2}{b^2}\right) \tag{20b}$$

The term I/Ω in Eq. (14) is the eigenfunction ϕ_{00}; therefore, the sums in Eqs. (6), (8), and (9) run from $k = 0$ to ∞ excluding the single term for which $k = m = 0$. Furthermore,

$$(\phi_{km}, \phi_{km}) = ab \qquad (k \neq 0, m \neq 0)\ , \tag{21a}$$

$$(\phi_{km}, \phi_{km}) = 2ab \qquad (k = 0 \text{ or } m = 0, \text{ but not both})\ . \tag{21b}$$

Thin Outer Ring. Imagine the region Ω_0 to be a strip of uniform thickness s just inside the outer boundary of the rectangle (see Fig. 4). In calculating (ϕ_{km}, g) for $k \neq 0$, $m \neq 0$, let us begin by considering the contribution of the trapezoid KACL. It is the contribution of the rectangle KBCL less the contribution of the triangle ABC. Similarly, the contribution of the trapezoid MACN is that of the rectangle MDCN less that of the triangle ADC. The contributions of the two rectangles KBCL and MDCN are zero, so that the total contribution from the first quadrant is from the square ABCD. Since the eigenfunction is even in both x and y, the contributions from all quadrants are the same; therefore (ϕ_{km}, g) is four times the contribution from the square ABCD, namely,

$$(\phi_{km}, g) = -4\int_{a-s}^{a} dx \cos\left(\frac{k\pi x}{a}\right)\int_{b-s}^{b} dy \cos\left(\frac{m\pi y}{b}\right) \tag{22a}$$

$$= -\frac{4ab}{km\pi^2}\sin\left[k\pi(1 - s/a)\right]\sin\left[m\pi\,(1 - s/b)\right]\ . \tag{22b}$$

When $s \to 0$, (ϕ_{km}, g) approaches 0 as $(-1)^{k+m+1}4s^2$. Thus the numerator in the summands in Eq. (9b) approaches 0 as s^4. The area Ω_0, on the other hand, approaches 0 as s, so the denominator in the summands in Eq. (9b) approaches 0 as s^2. Hence the limiting contribution to the right-hand side of Eq. (9b) from the eigenfunctions for which $k \neq 0$ and $m \neq 0$ is zero.

Now let us calculate (ϕ_{km}, g). In the first quadrant, the entire contribution comes from the rectangle MABN. As before, the total contribution is four times as great:

ORNL-DWG 91M-2912 FED

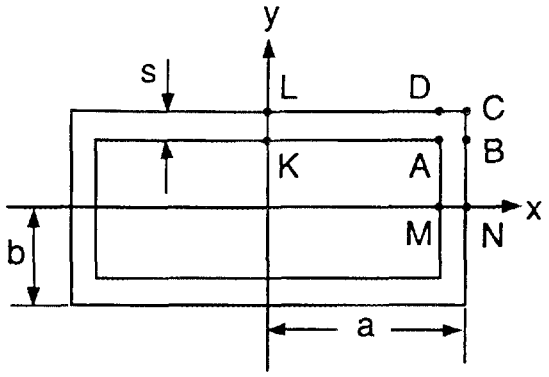

Fig. 4. A rectangular conductor with its initial current distribution in a strip of width s just inside the outer boundary of the rectangle.

$$(\phi_{k0}, g) = 4\int_{a-s}^{a} dx \cos\left(\frac{k\pi x}{a}\right) \int_0^{b-s} dy \tag{23a}$$

$$= -4\,(b-s)\left(\frac{a}{k\pi}\right) \sin\left[k\pi\,(1-s/a)\right] \ , \tag{23b}$$

which goes to zero as $(-1)^k\, 4bs$ as $s \to 0$. Similarly, the limiting contribution of (ϕ_{km}, g) is $(-1)^m\, 4as$ in the limit $\Omega_0 \sim 4(a+b)s$. Thus from Eq. (9b) we find

$$Q = \frac{\mu_0 I^2}{48(a+b)^2} \ . \tag{24}$$

When a, the source thickness in Eq. (13), goes to 0, Q approaches the value $\mu_0 I^2/24$, which is the limit for a slab with infinitely thin current sources at its outer faces. When a, the width in Eq. (24), is much greater than b, the length, Q approaches the value $\mu_0 I^2/12$, a value twice as great as the slab value. This is because letting the width of the rectangle greatly exceed its height does not eliminate the contribution from the ends at $x = \pm a$ any more than letting $h \to \infty$ in Eq. (13) makes Q approach zero. The value of Q given by Eq. (24) is the sum of two equal contributions, one from the horizontal pair of faces ($k = 0$ eigenfunctions) and one from the pair of vertical faces ($m = 0$ eigenfunctions). The individual contribution from each pair of faces approaches $\mu_0 I^2/24$, the slab limit, as it should.

If we compare Eq. (24) for a square (i.e., for $a = b$) with Eq. (17a) for a cylinder of equal area, we find that

$$\frac{Q_{\text{cyl}}}{Q_{\text{square}}} = \frac{3}{\pi} \ . \tag{25}$$

Rutherford Cable. A configuration of interest is a thin Rutherford cable at the center of a rectangular conductor (see Fig. 5). Owing to the symmetry of the

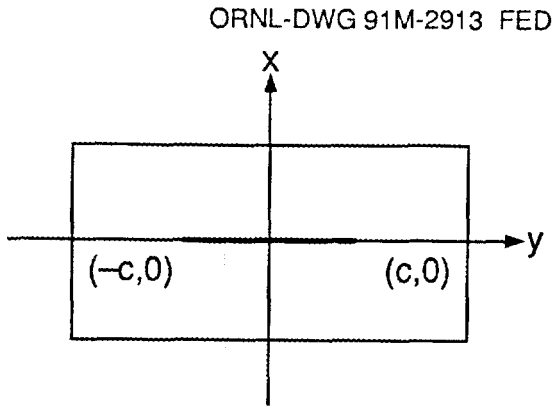

Fig. 5. A rectangular conductor with a thin Rutherford cable centrally placed.

configuration, we can again use the eigenfunctions and eigenvalues of Eqs. (20a) and (20b) excluding the term $k = m = 0$. The terms in the sum Eq. (9b) are now of three kinds: (i) $k = 0$, $m \neq 0$; (ii) $k \neq 0$, $m = 0$; and (iii) $k \neq 0$, $m \neq 0$. For terms of type (i), $\alpha_{km}^2 = \pi^2 m^2/b^2$, $(\phi_{km}, \phi_{km}) = 2ab$, and $(\phi_{km}, g)/\Omega_0 = 1$ if we neglect the transverse thickness of the cable. The contribution of these terms to the right-hand side of Eq. (9b) is then

$$Q_{(i)} = \frac{\mu_0 (I/2a)^2}{24} \quad . \tag{26}$$

For terms of type (ii), $\alpha_{km}^2 = \pi^2 k^2/a^2$, $(\phi_{km}, \phi_{km}) = 2ab$, and $(\phi_{km}, g)/\Omega_0 = \sin(k\pi c/a)/(k\pi c/a)$. The contribution of these terms to the right-hand side of Eq. (9b) is

$$Q_{(ii)} = \frac{\mu_0 (I/2a)^2}{24} \left(\frac{a}{b}\right)^2 \left(1 - \frac{c}{a}\right)^2 . \tag{27}$$

Finally, for terms of type (iii), $\alpha_{km}^2 = \pi^2 (k^2/a^2 + m^2/b^2)$, $(\phi_{km}, \phi_{km}) = ab$, and $(\phi_{km}, g)/\Omega_0 = \sin(k\pi c/a)/(k\pi/a)$. The contribution of these terms to the right-hand side of Eq. (9b) is

$$Q_{(iii)} = \frac{\mu_0 (I/2a)^2}{24} G \quad , \tag{28a}$$

where

$$G = \frac{12}{\pi^2} \sum_{k=1}^{\infty} \left[\frac{\sin(k\pi c/a)}{(k\pi c/a)}\right]^2 \sum_{m=1}^{\infty} \frac{1}{m^2 + (kb/a)^2} \quad . \tag{28b}$$

According to Jolley,[8]

$$\sum_{m=1}^{\infty} (m^2 + x^2)^{-1} = [\pi x \coth(\pi x) - 1]/2x^2 \ , \tag{29}$$

so that finally the geometric factor G becomes

$$G = 6 \sum_{k=1}^{\infty} \left[\frac{\sin k\pi c/a}{(k\pi c/a)} \right]^2 H(k\pi b/a), \tag{30a}$$

where

$$H(x) = (x \coth x - 1)/x^2 \ . \tag{30b}$$

The series (30) can be summed numerically and converges rapidly. Shown in Fig. 6 is Q plotted vs c/a for various values of b/a.

A similar calculation for an initial current source region confined to the rectangle $-p < x < p$, $-q < y < q$ gives the result

$$Q = \frac{\mu_0 I^2}{4ab} \cdot \frac{1}{24} \left[\frac{a}{b}\left(1 - \frac{p}{a}\right)^2 + \frac{b}{a}\left(1 - \frac{q}{b}\right)^2 \right.$$

$$\left. + \frac{12}{\pi^2} \sum_{k=1}^{\infty} \sum_{m=1}^{\infty} \left[\frac{\sin(k\pi p/a)}{(k\pi q/a)} \cdot \frac{\sin(m\pi q/b)}{(m\pi q/b)} \right]^2 \frac{ab}{k^2 b^2 + m^2 a^2} \right] . \tag{30c}$$

The series (30c), though a double series, converges rapidly enough to allow easy numerical summation.

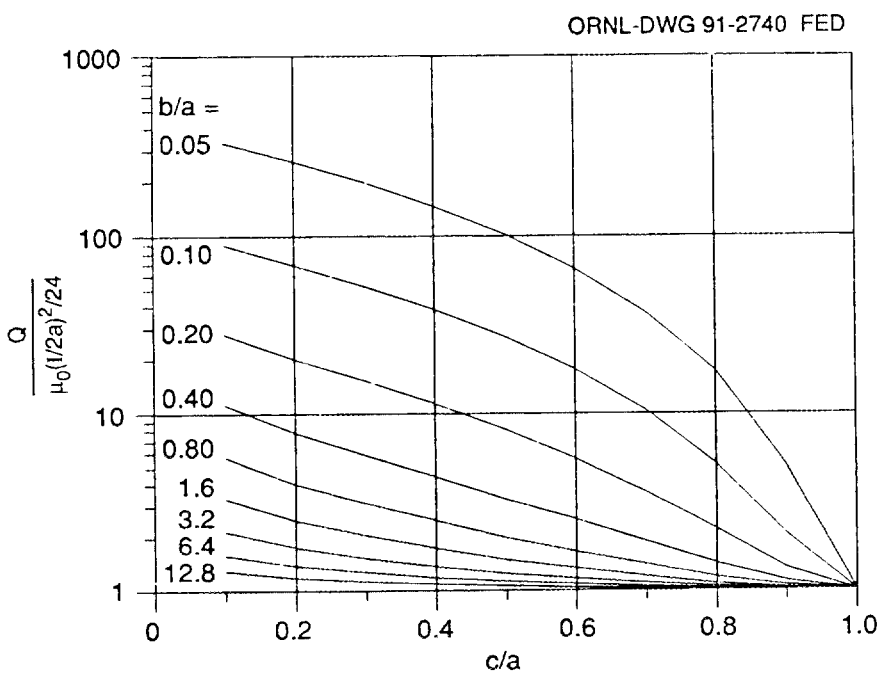

Fig. 6. The excess heat density Q for the conductor of Fig. 5 divided by $\mu_0(I/2a)^2/24$ as a function of c/a for various values of b/a.

REFERENCES

1. C. A. Luongo, R. J. Loyd, and C. L. Chang, "Current Diffusion Effects on the Performance of Large Monolithic Conductors," *IEEE Trans. Magn.* **25** (2), 1576–81 (1989).

2. T. Mito, J. Yamamoto, K. Takahata, N. Yanagi, O. Motojima, and the LHD Design Group, "Development of Superconducting Conductors for Large Helical Device," *IEEE Trans. Magn.* **27** (2), 2224–27 (1991).

3. X. Huang, Y. M. Eyssa, and M. A. Hilal, "High Current Density Aluminum Stabilized Conductor Concepts for Space Applications," *IEEE Trans. Magn.* **25** (2), 1535–37 (1989).

4. X. Huang and Y. M. Eyssa, "Stability of Large Composite Superconductors," *IEEE Trans. Magn.* **27** (2), 2304–7 (1991); J. M. Pfotenhauer, M. K. Abdelsalam, F. Bodker, D. Huttleston, Z. Jiang, O. D. Lokken, D. Scherbarth, B. Tao, and D. Yu, "Test Results from the SMES Proof of Principle Experiment," *IEEE Trans. Magn.* **27** (2), 1704–7 (1991).

5. Lawrence Dresner, "Propagation of Normal Zones of Finite Size in Large, Composite Superconductors," in *Proceedings of the Eleventh International Conference on Magnet Technology (MT-11) Held in Tsukuba, Japan, August 28–September 2, 1989,* ed. T. Sekiguchi and S. Shimamoto, Elsevier Applied Science, New York, 1990, pp. 1084–9.

6. R. Kupferman, R. G. Mints, and E. Ben-Jacob, "Dynamics of Normal Zone in Large Composite Superconductors," submitted to *Applied Physics Letters.*

7. See, for example, H. Margenau and G. M. Murphy, *The Mathematics of Physics and Chemistry,* D. van Nostrand, New York, 1943, pp. 259 and 329; or see R. Courant and D. Hilbert, *Methods of Mathematical Physics,* Vol. I, Interscience, New York, 1953, p. 293.

8. L. B. W. Jolley, *Summation of Series*, Dover, New York, 1961, #343.

Appendix A
CALCULATION FOR EQ. (12)

In order to verify the trigonometric sum

$$\frac{6}{\pi^2}\sum_{k=1}^{\infty}\frac{1}{k^2}\left[\frac{\sin(\pi kx)}{\pi kx}\right]^2 = (1-x)^2 \qquad (0 < x < 1)\ , \tag{A1}$$

we must first eliminate the square of the sine using the identity

$$\sin^2 y = \frac{1}{2}(1 - \cos 2y). \tag{A2}$$

Then after some straightforward rearrangement, we obtain

$$\frac{3}{\pi^4}\sum_{k=1}^{\infty}\frac{\cos(2\pi kx)}{k^4} = \frac{1}{30} - x^2(1-x)^2. \tag{A3}$$

In obtaining Eq. (A3) we have used the relation

$$\sum_{k=1}^{\infty}\frac{1}{k^4} = \frac{\pi^4}{90}, \tag{A4}$$

which can be found in Ref. 1. Equation (A4) is a Fourier series, and the coefficients on the left-hand side can be found, after quite a lengthy calculation, from Euler's formulas.

REFERENCE

1. L. B. W. Jolley, *Summation of Series*, Dover, New York, 1961, #343.

Appendix B
CALCULATION FOR EQ. (17a)

The sum in Eq. (17a) can be evaluated by a technique due to Euler and described by Polya.[1] Euler begins by considering polynomials $P(z)$ of order n whose roots are r_1, r_2, ..., r_n. In our case we shall specialize to even polynomials of order $2n$, so that each of the roots $r_1, r_2, ..., r_n$ is a double root. Then, following Euler, we can write

$$P(z)/P(0) = \left(1 - z^2/r_1^2\right)\left(1 - z^2/r_2^2\right) \ldots \left(1 - z^2/r_n^2\right) \tag{B1a}$$

$$= 1 - z^2 \sum_{k=1}^{n} \frac{1}{r_k^2} + \ldots \tag{B1b}$$

so that

$$\sum_{k=1}^{n} \frac{1}{r_k^2} = -\frac{\ddot{P}(0)}{2P(0)}. \tag{B2}$$

In his use of this formula, Euler applies it to functions that can be represented as a Maclaurin series. If we do this as well and apply it to the function $P(z) = J_1(z)/z$, we find at once that

$$\sum_{k=1}^{\infty} 1/\gamma_k^2 = 1/8.$$

REFERENCE

1. G. Polya, *Induction and Analogy in Mathematics,* vol. 1, Princeton Univ. Press, Princeton, N.J., 1954, pp. 18–21.

Appendix C
CALCULATION FOR EQ. (18)

The second factor on the right-hand side of Eq. (18) can be written

$$\frac{2}{\pi^2}\sum_{k=1}^{\infty}\left[\frac{J_1(\gamma_k r)}{\gamma_k r}\right]^2\frac{1}{\gamma_k^2 J_0^2(\gamma_k)}, \tag{C1}$$

where $r = R_2/R$. When $r << 1$, the quantity in the square brackets is close to 1/2 until γ_k becomes roughly $1/r$. Now for large γ_k, $J_0(\gamma_k)$ is given closely by $\sqrt{2/\pi\gamma_k}$, so that the first $1/r$ terms of the sum in Eq. (18) become

$$\frac{1}{4\pi}\sum_{k=1}^{1/r}\frac{1}{\gamma_k}. \tag{C2}$$

Since the roots γ_k are asymptotically spaced at intervals of π, we can estimate the sum in Eq. (C2) by the integral

$$\frac{1}{4\pi^2}\int_{\gamma_1}^{1/r}\frac{d\gamma}{\gamma} = \frac{1}{4\pi^2}\left[\ln\left(\frac{1}{r}\right) - \ln\gamma_1\right] \sim \frac{1}{4\pi^2}\ln\left(\frac{1}{r}\right), \tag{C3}$$

which is the estimate we are seeking.

ORNL/TM-11827
Dist. Category UC-220

INTERNAL DISTRIBUTION

1. C. C. Baker
2. L. A. Berry
3. B. A. Carreras
4. R. A. Dory
5. J. L. Dunlap
6. H. H. Haselton
7–16. L. Dresner
17. M. S. Lubell
18. R. A. Phaneuf
19. M. J. Saltmarsh
20. J. Sheffield
21. R. P. Leinius
22–23. Laboratory Records Department
24. Laboratory Records, ORNL-RC
25–26. Central Research Library
27. Document Reference Section
28. Fusion Energy Division Library
29–30. Engineering Technology/Fusion Energy Division Publications Office
31. ORNL Patent Office

EXTERNAL DISTRIBUTION

32. Office of the Assistant Manager for Energy Research and Development, U.S. Department of Energy, Oak Ridge Operations Office, P.O. Box E, Oak Ridge, TN 37831
33. J. D. Callen, Department of Nuclear Engineering, University of Wisconsin, Madison, WI 53706-1687
34. R. W. Conn, Department of Chemical, Nuclear, and Thermal Engineering, University of California, Los Angeles, CA 90024
35. N. A. Davies, Acting Director, Office of Fusion Energy, Office of Energy Research, ER-50 Germantown, U.S. Department of Energy, Washington, DC 20545
36. S. O. Dean, Fusion Power Associates, Inc., 2 Professional Drive, Suite 248, Gaithersburg, MD 20879
37. H. K. Forsen, Bechtel Group, Inc., Research Engineering, P.O. Box 3965, San Francisco, CA 94119
38. R. W. Gould, Department of Applied Physics, California Institute of Technology, Pasadena, CA 91125
39. R. A. Gross, Plasma Research Laboratory, Columbia University, New York, NY 10027
40. D. M. Meade, Princeton Plasma Physics Laboratory, P.O. Box 451, Princeton, NJ 08543
41. M. Roberts, International Programs, Office of Fusion Energy, Office of Energy Research, ER-52 Germantown, U.S. Department of Energy, Washington, DC 20545
42. W. M. Stacey, School of Nuclear Engineering and Health Physics, Georgia Institute of Technology, Atlanta, GA 30332
43. D. Steiner, Nuclear Engineering Department, NES Building, Tibbetts Avenue, Rensselaer Polytechnic Institute, Troy, NY 12181
44. R. Varma, Physical Research Laboratory, Navrangpura, Ahmedabad 380009, India
45. Bibliothek, Max-Planck Institut für Plasmaphysik, Boltzmannstrasse 2, D-8046 Garching, Federal Republic of Germany
46. Bibliothek, Institut für Plasmaphysik, KFA Jülich GmbH, Postfach 1913, D-5170 Jülich, Federal Republic of Germany
47. Bibliothek, KfK Karlsruhe GmbH, Postfach 3640, D-7500 Karlsruhe 1, Federal Republic of Germany

48. Bibliotheque, Centre de Recherches en Physique des Plasmas, Ecole Polytechnique Fédérale de Lausanne, 21 Avenue des Bains, CH-1007 Lausanne, Switzerland
49. J. Tachon, CEN/Cadarache, Departement de Recherches sur la Fusion Controllée, F-13108 Saint-Paul-lez-Durance Cedex, France
50. Bibliothèque, CEN/Cadarache, F-13108 Saint-Paul-lez-Durance Cedex, France
51. Library, Culham Laboratory, UKAEA, Abingdon, Oxfordshire, OX14 3DB, England
52. Library, JET Joint Undertaking, Abingdon, Oxfordshire OX14 3EA, England
53. Library, FOM-Instituut voor Plasmafysica, Rijnhuizen, Edisonbaan 14, 3439 MN Nieuwegein, The Netherlands
54. Library, National Institute for Fusion Science, Chikusa-ku, Nagoya 464-01, Japan
55. Library, International Centre for Theoretical Physics, P.O. Box 586, I-34100 Trieste, Italy
56. Library, Centro Richerche Energia Frascati, C.P. 65, I-00044 Frascati (Roma), Italy
57. Library, Plasma Physics Laboratory, Kyoto University, Gokasho, Uji, Kyoto 611, Japan
58. Plasma Research Laboratory, Australian National University, P. O. Box 4, Canberra, A.C.T. 2601, Australia
59. Library, Japan Atomic Energy Research Institute, Naka Fusion Research Establishment, 801-1 Mukoyama, Naka-machi, Naka-gun, Ibaraki-ken, Japan
60. G. A. Eliseev, I. V. Kurchatov Institute of Atomic Energy, P.O. Box 3402, 123182 Moscow, U.S.S.R.
61. V. A. Glukhikh, Scientific-Research Institute of Electro-Physical Apparatus, 188631 Leningrad, U.S.S.R.
62. I. Shpigel, Institute of General Physics, U.S.S.R. Academy of Sciences, Ulitsa Vavilova 38, Moscow, U.S.S.R.
63. D. D. Ryutov, Institute of Nuclear Physics, Siberian Branch of the Academy of Sciences of the U.S.S.R., Sovetskaya St. 5, 630090 Novosibirsk, U.S.S.R.
64. O. Pavlichenko, Kharkov Physical-Technical Institute, Academical St. 1, 310108 Kharkov, U.S.S.R.
65. Deputy Director, Southwestern Institute of Physics, P.O. Box 15, Leshan, Sichuan, China (PRC)
66. Director, The Institute of Plasma Physics, P.O. Box 26, Hefei, Anhui, China (PRC).

67–78. Given distribution as shown in DOE/OSTI-4500-R75, Electric Energy Systems (Category Distribution UC-220) (12 copies)